

**An analysis of the self-excited torsional vibrations  
of the electromechanical drive system**

Robert KONOWROCKI and Tomasz SZOLC

*Institute of Fundamental Technological Research of the Polish Academy of Sciences  
ul. A. Pawińskiego 5B, 02-106 Warszawa, rkonow@ippt.pan.pl, tszolc@ippt.pan.pl*

**Abstract**

This paper presents a dynamic analysis of torsional vibrations of the railway drive system. A dynamic electromechanical drive model has been created and then integrated with the railway wheelset-rail system to simulate self-excited torsional vibrations of the considered system. Results of this analysis are used in order to investigate the drive system's sensitivity to torsional oscillations. Here, the dynamic electromechanical interaction between the electric driving motor and the rotating wheelset is considered. This investigation has proved that the torsional stiffness and damping of drivetrain system strongly affect amplitudes of the self-excited vibrations. A self-excited vibrations affecting on an energy consumption of the electric motor of the considered system are studied

**Keywords:** torsional vibrations, electromechanical coupling, wheel-rail adhesion, wheelset drivetrain dynamic

**1. Introduction**

Mechanical vibrations and deformations are phenomena associated with an operation of majority of railway vehicle drivetrain structures. The knowledge about torsional vibrations in transmission systems of railway vehicles is of a great importance in the fields dynamics of mechanical systems [1]. Torsional vibrations in the railway vehicle drive train are generated by several phenomena. Generally, these phenomena are very complex and they can be divided into two main parts. To the first one belongs the electromechanical interaction between of the railway drive system including the: electric motor, gears, the driven part of disc clutch and driving parts of the gear clutch [2]. To the second one belong torsional vibrations of the flexible wheels [3,4] and wheelsets caused by variation of adhesion forces in the wheel-rail contact zone [5]. An interaction of the adhesion forces has nonlinear features which are related to the creep value and strongly depends on the wheel-rail zone condition and track geometry (when driving on a curve section of the track). In many modern mechanical systems torsional structural deformability plays an important role. Often the study of railway vehicle dynamics using the rigid multibody methods without torsionally deformable elements are used [6]. This approach does not allow to analyse self-excited vibrations which have an important influence on the wheel-rail longitudinal interaction [7].

A dynamic modelling of the electrical drive systems coupled with elements of a driven machine or vehicle is particularly important when the purpose of such modelling is to obtain an information about the transient phenomena of system operation, like a run-up, run-down and loss of adhesion in the wheel-rail zone. In this paper most attention is paid to the modelling of an electromechanical interaction between the electric driving motor and the railway wheelset as well as to an influence of the self-excited torsional vibrations in the considered drive system.

## 2. Mathematical modeling of the wheelset and the electric motor

In order to investigate a character of self-excited torsional vibrations in the electric railway vehicle powertrain and a dynamic mutual coupling between the wheelset and the electric motor, a possibly realistic and reliable electromechanical model of the railway drivetrain is applied. The mechanical drive system is represented by a torsionally vibrating system of four-DOFs. The scheme of the considered model is shown in Figure 1.

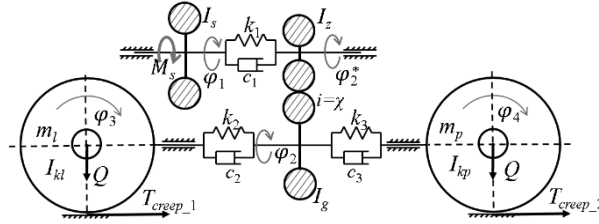


Fig. 1. Scheme of the dynamic model of the railway wheelset drive system

A mathematical model of the single torsionally deformable railway wheelset under torsional vibrations induced by the traction motor and various adhesion frictional effects occurring in wheel-rail contact zones has been derived by means of the second-order Lagrange's equations in the generalized coordinates  $\varphi_i(t)$ . These coordinates describe angular displacements of the drivetrain components of the wheelset. Here, there will be presented a torsional dynamic analysis of the single wheelset running on a geometrically perfect straight section under various operational conditions determined by longitudinal slip  $s_i$  of both wheels, vertical wheel forces  $Q+m \cdot g$  and vehicle velocity  $v$ . The drive torque and the retarding one due to the creep of the rails with the wheels complements the conservative railway drive model on the right side (1) and it can be expressed as

$$\mathbf{I}\ddot{\varphi}(t) = (\mathbf{K}_{wheelset} + \mathbf{K}_{gear})\varphi(t) + (\mathbf{C}_{wheelset} + \mathbf{C}_{gear})\dot{\varphi}(t) = \mathbf{M}_{drive} - \mathbf{M}_{creep}, \quad (1)$$

where  $\mathbf{I}$  denotes the mass matrix containing mass moments of inertia of rotating elements of the drive system, the matrices  $\mathbf{K}_{wheel}$ ,  $\mathbf{K}_{gear}$ ,  $\mathbf{C}_{wheel}$  and  $\mathbf{C}_{gear}$  express the torsional stiffness and damping properties of the wheelset, disc-clutch and of the gearbox wheel, respectively. Vector  $\mathbf{M}_{drive}$  contains the electromagnetic torque generated by an asynchronous motor described in the following part of the paper and vector  $\mathbf{M}_{creep}$  contains the traction torque generated by longitudinal tangential loads in the wheel-rail zones. Their form can be expressed as

$$T_{creep\_i} = \mu_i(s_i) \cdot (Q + m_i g), \quad i = 1, 2, \quad (2)$$

where  $Q$  is the normal load imposed on the single wheel,  $r$  is the wheel radius and  $\mu(s_i)$  is the traction coefficient expressed in Eq. (4). Its maximum value is called an adhesion coefficient. The longitudinal creepage of the wheels is defined in the following form

$$s_0 = \left( \frac{3.6\omega_i r}{v} - 1 \right), \quad s_i = s_0 + \left( \frac{3.6\dot{\varphi}_i r}{v} - 1 \right), \quad i = 1, 2, \quad (3)$$

where  $s_0$  and  $s_i$  are the longitudinal creepage before and during disturbances, respectively. Symbol  $\omega_i$  is the angular speed of the  $i$ -th wheel,  $i$ -index means the left and the right wheel and  $v$  denotes forward wheelset velocity in km/h obtained by the equivalent angular speed of wheelset axle  $\dot{\phi}_2$  at the contact point.

In equation (1) the traction torque including torques  $M_{creep_{1,2}}$  on left and right wheel of the wheelset have nonlinear properties. These properties are dependent on a profile of adhesion characteristic describing a contact in the wheel-rail zones. Depending on the adopted various maintenance, operation and weather conditions, this characteristic can take into consideration various forms of creepage curves, as shown in Fig. 2. The creepage curve applied for the carried out investigations has been plotted in Fig. 3 and it can be expressed by the following equation

$$\mu(s_i) = 0.3 * [(a + \exp(-s_i) + \tanh(\frac{b}{c} \cdot s_i) / 2 + (d \cdot \text{atan}(e \cdot s_i)) + \exp(f \cdot s_i))], \quad i = 1, 2. \quad (4)$$

For dry and wet weather conditions in the wheel-rail zone parameters of Eq. 4 have numerical values contained in Table 1.

Table 1. Parameters for traction coefficient in Eq. (4)

Quantity	a	b/c	d	e	f
dry	-1	100	1.75	0.7	-7
wet	-2	25	1.25	1	-0.5

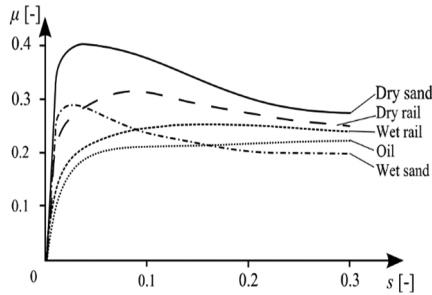


Fig. 2. Adhesion-creep characteristic of the railway conditions [8]

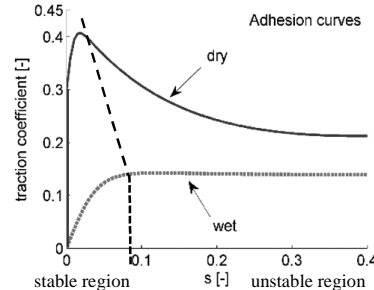


Fig. 3. Profile of adhesion curves used in investigations

The adhesion curve can be divided into two regions, see Fig. 3. The first region is characterized by a rapidly rising slope of the curve is the stable region. The second one, due to a negative damping results in visible decreasing slope, can lead to self-excited oscillations in the wheel-rail contact zone. This phenomenon makes the driven wheelset slipping on the rails of a railway track. Consequently, when a tangential force between the wheel and the rail exceeds an adhesion force in the wheel-rail contact zone, the self-excited torsional vibrations of the wheelset occur. Such a phenomenon has a very large impact on the relative rotation between the wheel and the axle due to a lack of friction in press fitting [9] and it can make vehicle derailed. Additional dynamic torsional overloads produce disturbances in the wheelset drive system, which has a influence on the traction moment of a railway vehicle. This characteristic of the traction moment is also dependent on electrical parameters of the motor, power supply and its regulation. A modeling of the

electrical part of a drivetrain is a very difficult and complex task. For a simple solution it is possible to use a linearization around of the working point static characteristic of the driving motor. But, in the case of a more advanced analysis of transient phenomena in the drivetrain an accurate circuit model of the electric motor is needed [10,11]. The asynchronous motors are very commonly applied as railway vehicles driving sources. From the viewpoint of electromechanical coupling investigation, for an introductory approach the properly advanced circuit model of the electric motor seems to be required, similarly as e.g. in [12]. In the case of the symmetrical three-phase asynchronous motor electric current oscillations in its windings are described by the six circuit voltage equations. In order to simplicity of their form they are transformed into the system of four Park's equations in the so called ' $\alpha\beta$ -dq' reference system

$$\begin{bmatrix} \sqrt{\frac{3}{2}}U \cos(\omega_e t) \\ \sqrt{\frac{3}{2}}U \sin(\omega_e t) \\ 0 \\ 0 \end{bmatrix} = \begin{bmatrix} L_s + \frac{1}{2}L_m & 0 & \frac{3}{2}L_m & 0 \\ 0 & L_s + \frac{1}{2}L_m & 0 & \frac{3}{2}L_m \\ \frac{3}{2}L_m & 0 & L_r' + \frac{1}{2}L_m & 0 \\ 0 & \frac{3}{2}L_m & 0 & L_r' + \frac{1}{2}L_m \end{bmatrix} \begin{bmatrix} i_{\alpha}^s(t) \\ i_{\beta}^s(t) \\ i_d^r(t) \\ i_q^r(t) \end{bmatrix} + \begin{bmatrix} R_s & 0 & 0 & 0 \\ 0 & R_s & 0 & 0 \\ 0 & \frac{3}{2}pL_m\dot{\varphi}_1(t) & R_r & p\dot{\varphi}_1(t)(L_r' + \frac{1}{2}L_m) \\ -\frac{3}{2}pL_m\dot{\varphi}_1(t) & 0 & -p\dot{\varphi}_1(t)(L_r' + \frac{1}{2}L_m) & R_r \end{bmatrix} \begin{bmatrix} i_{\alpha}^s(t) \\ i_{\beta}^s(t) \\ i_d^r(t) \\ i_q^r(t) \end{bmatrix}, \quad (5)$$

where  $U$  denotes the power supply voltage,  $\omega_e$  is the supply voltage circular frequency,  $L_s, L_r'$  are the stator coil inductance and the equivalent rotor coil inductance, respectively,  $L_m$  denotes the relative rotor-to-stator coil inductance,  $R_s, R_r$  are the stator coil resistance and the equivalent rotor coil resistance, respectively,  $p$  is the number of pairs of the motor magnetic poles,  $\dot{\varphi}_1(t)$  is the current rotor angular speed including the average and vibratory component and  $i_{\alpha}^s, i_{\beta}^s$  are the electric currents in the stator windings reduced to the electric field equivalent axes  $\alpha$  and  $\beta$  and  $i_d^r, i_q^r$  are the electric currents in the rotor windings reduced to the electric field equivalent axes  $d$  and  $q$ , [12]. Then, the electromagnetic torque generated by such a motor can be expressed by the following formula

$$M_s = \frac{3pL_m(i_{\beta}^s \cdot i_d^r - i_{\alpha}^s \cdot i_q^r)}{2}. \quad (6)$$

In our approach the interaction between the electromagnetic and mechanical systems of the considered powertrain coupled mutually through electromagnetic torque  $M_s$  and angular rotor velocity  $\dot{\varphi}_1$  is shown in Eqs. (5) and (6). In order to control the electric motor assumed in the applied drive system model the field-oriented control methods has been used [13]. According to the above, this set of coupled electromechanical Eqs. (1), (5) and (6) is going to be simultaneously solved by means of a selected direct integration method for electric parameters including: resistance of the stator and the rotor equal  $R_s=0.288 \Omega$ ,  $R_r=0.158 \Omega$ . The relative inductance, inductance of the stator windings and

inductance of the rotor windings are respectively equal to  $L_m = 0,0412$  H,  $L_s = 0,0425$  H and  $L_r = 0,0418$  H. The asynchronous motor has 4 pole pairs and its supply voltage is equal to 3 kV with 60 Hz supply frequency. In the considered case, the Runge-Kutta fourth-order method will be applied for motion equations of the electromechanical model assumed in this way.

### 3. Numerical results

In the computational example railway drivetrain system with the torsionally flexible wheelset is used as an object of considerations. This wheelset of a total weight 1500 kg and a load of the single wheel equal to  $Q=40$  kN is driven by the asynchronous motor by means of the disc-clutch with torsional stiffness and damping coefficient  $k_1=3000$  kNm,  $c_1=100$  Ns/m. The spur gear stage of the ratio  $i=1:6$  reduces a rotational speed of the wheelset into  $\dot{\varphi}_2^* = \dot{\varphi}_2 \cdot \chi$ . There is assumed that the minimum radius of the wheelset axle and the half of length of the axle are respectively equal to 0.08 and 0.75 m. This axle is made of steel P35G. The torsional stiffness of this axis has been determined equal to  $k_2=k_3= 6.9e7$  Nm/rad. More parameters applied in this investigations are also given in the Table 2.

Table 2 Simulation base parameters

$\chi$	$c_2$	$c_3$	$I_s$	$I_z$	$I_g$	$I_{kl}$	$I_{kr}$
0.16	50 Ns/m	50 Ns/m	2.1 kgm <sup>2</sup>	20.2 kgm <sup>2</sup>	43 kgm <sup>2</sup>	78 kgm <sup>2</sup>	78 kgm <sup>2</sup>

The simulation model described above can be used to simulate several different conditions of operation, i.e. motor acceleration, deceleration, load change, fault condition, etc. However, due the limited size, only selected results are presented here. An amplitude of self-excited vibrations is an important evaluating indicator to measure the vibration magnitude. Some drive system parameters influencing the amplitude of the self-excited torsional vibration are shown in Figs. 4 and 5. Figure 4a and 4c present the result of the self-excited vibration amplitudes and the spectrum of them at various damping between the drivetrain system and the wheelset wheels. As shown in this figure, the vibration amplitude decreases with an increase of damping level where the dominant frequency of the vibration is kept constant. An increase of the damping can restrain this amplitude and shorten the convergence time of the torsional vibrations, but it is not affected whether the self-excited vibration occurs or not. The same effect can be observed on time-histories of the currents of the stator windings shown in Figs. 4b and 4 d. Figure 5a shows a result of the self-excited vibration amplitudes at different equivalent stiffness between the drivetrain and the wheelset wheels of wheelset.

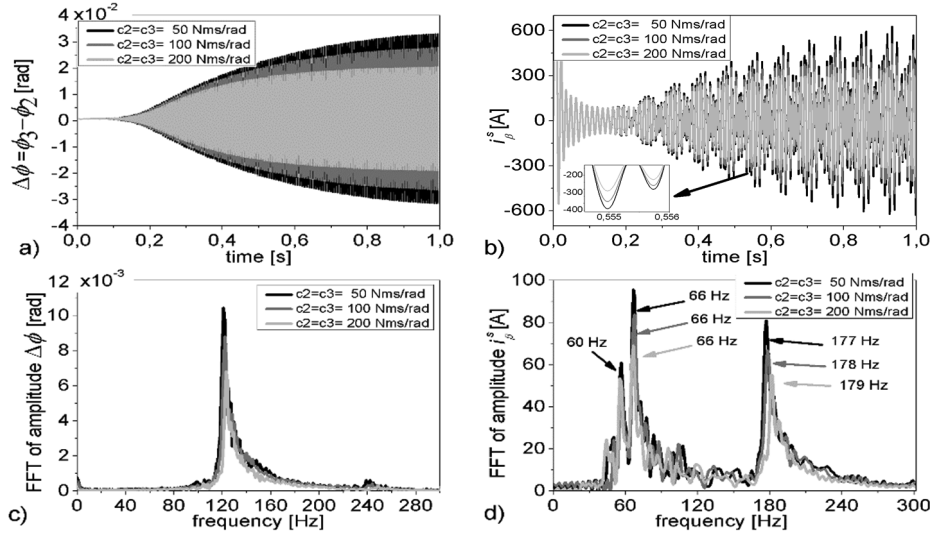


Fig. 4. Self-excited torsional vibration amplitudes of the mechanical and electric parameters at various torsional damping of wheelset drivetrain. Time-history (a) and amplitude spectrum (c) of the difference between the angular displacements of the left and right wheelset wheel. Time-history (b) and amplitude spectrum (d) of the electric currents in the stator winding

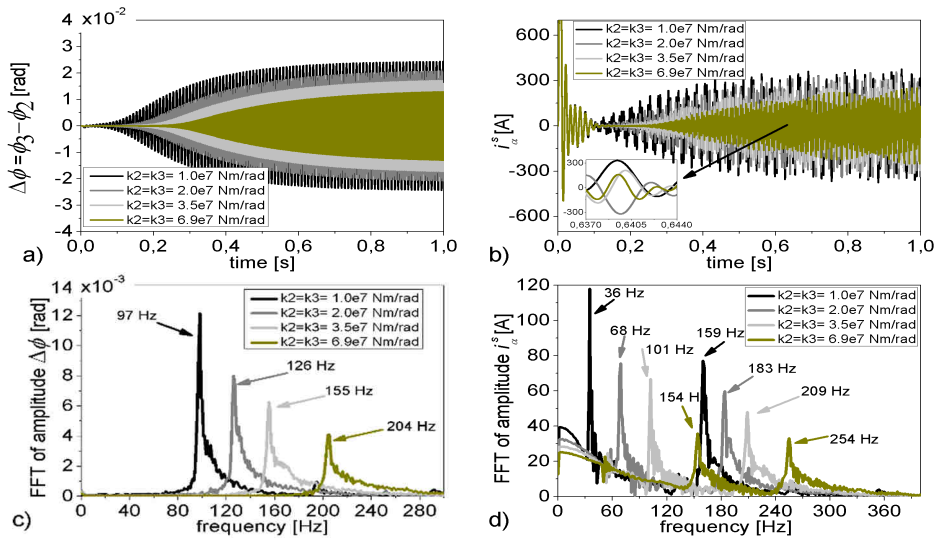


Fig. 5. Self-excited torsional vibration amplitudes of the mechanical and electric parameters at various torsional stiffness of wheelset drivetrain. Time-history (a) and amplitude spectrum (c) of the difference between the angular displacements of the left and right wheelset wheel. Time-history (b) and amplitude spectrum (d) of the electric currents in the stator winding

As shown in this figure (Fig 5.), the vibration amplitude decreases with an increase of  $k_2$  and  $k_3$ . It indicates that where increasing the torsional stiffness of drivetrain system, it is influences on the stability of the vibration and its shifting dominant frequency of the vibration in the higher range of the spectrum (Fig. 5c).

Considering the electrical parameter values of motor obtained from the above investigations it is worth highlighting that the self-excitation torsional vibrations affected on the entire electromechanical drivetrain system and they have a significant influence on the amount of theoretically expected electric energy  $P_{el}$  consumed by the driving motor. In the case of the investigated system, this energy can be determined by the electromotive forces induced in the asynchronous motor phases by voltages and currents in the stator windings. This energy can be defined [7].

$$P_{el} = \frac{1}{t_k} \int_0^{t_k} [U_{ds}(t) \cdot i_{\alpha}^s(t) + U_{qs}(t) \cdot i_{\beta}^s(t)] dt \quad (7)$$

where  $U_{ds}(t) = \sqrt{\frac{3}{2}}U \cos(\omega_e t)$ ,  $U_{qs}(t) = \sqrt{\frac{3}{2}}U \sin(\omega_e t)$ , and  $i_{\alpha}^s(t)$ ,  $i_{\beta}^s(t)$ , denote the voltages and currents in the stator circuits of the electric motor phases transformed into the reference system of Park's equations,  $t_k$  is the total duration time of the each variant of an analysis and the remaining symbols have been already defined in Eqs. (5) and (6). Table 3 illustrates the amounts of electric energy consumed by the drivetrain motor during the considered test scenarios at various of parameters the drive system discussed above.

Table 3. Amounts of electric energy consumed by the asynchronous motor during the assumed four scenarios of the investigation using the assumed drivetrain models

stiffness of drivetrain [Nm/rad]	1e7	2e7	3.5e7	6.9 e7
stiffness-energy consumed [kWs]	62,35	70,44	76,65	78,93
damping of drivetrain [Nms/rad]	50,00	100,00	150,00	200,00
damping-energy consumed [kWs]	78,93	88,37	88,59	93,02

From a comparison of the results shown in Table 3 it follows that, when the torsional stiffness increase, more electric energy have been consumed. This fact can be substantiated by change amplitude of the time-histories of the difference between the angular displacements of the left and right wheelset wheel characteristics of presented in Fig. 5.

#### 4. Final remarks and preview

In this paper, an electromechanical model of the railway vehicle drive system has been performed. This model has been used to investigate self-excited torsional vibrations occurring in this system. In the investigations their influence of the torsional vibration on the electric parameters of the drive motor are also considered. From obtained results it follows that a reduction of the self-excited vibration amplitudes by means of increasing the damping and stiffness between the driving motor and the wheelset and torsion stiffness of wheelset occur. The results obtained using numerical simulations indicated that the self-

excited torsional vibrations in the considered drive system are strongly dependent on the characteristics of the adhesion coefficient in wheel-rail contact zone. A circuit model of the electric motor in the considered drive system enable us to obtain values of electrical parameter characterizing the driving motor. The information concerning a frequency variation of the current in the driving motor stator can be used for monitoring and identification of self-excited vibration in the wheelset drivetrain system. The further work will be denoted to an assumption of the vehicle model with the drivetrain system and it will be carried out experimentally verification on real railway vehicle.

### References

1. R. Bogacz, T. Szolc, H. Irretier, *An application of torsional wave analysis to turbogenerator rotor shaft response*, J.Vibr. Acou. -Trans. of the Asme, Vol. 114-2 (1992) 149-153.
2. O. Ahmedov, V. Zeman, M. Byrtus, *Modelling of vibration and modal properties of electric locomotive drive*, Eng. Mech., Vol. 19: 2/3 (2012) 165–176.
3. S. Noga, R. Bogacz, T. Markowski, *Vibration analysis of a wheel composed of a ring and a wheel-plate modelled as a three-parameter elastic foundation*, J.Sound Vib., Vol. 333:24, (2014) 6706-6722.
4. R. Bogacz, R. Konowrocki, *On new effects of wheel-rail interaction*, Arch. Appl. Mech, Vol.82 (2012)1313-1323.
5. V. Zeman, Z. Hlavac, *Dynamic wheelset drive load of the railway vehicle caused by shortcircuit motor moment*, App. & Comp. Mech., Vol.3, No.2 (2009)423–434.
6. B.S. Branislav, *Simulation of torsion moment at the wheel set of the railway vehicle with the traction electromotor for wavy direct current*, Mech. Trans. Com., Issue 3 (2008) 6-9
7. J. Liu, H. Zhao, W. Zhai, *Mechanism of self-excited torsional vibration of locomotive driving system*, Front. Mech. Eng.China, Vol.5:4 (2010,) 465-469.
8. A.K. Kumar, *Method and system of limiting the application of sand to a railroad rail*, U.S. Patent 7,290,870B2, Nov. 6, (2007).
9. S. Friedrich, M. Traupe, *Dynamic Torsional Loads on Wheelsets. Recent Findings for the Assessment*, Fatigue Strength and Simulation, T.TVI 24, Milan (2014).
10. T. Szolc, R. Konowrocki, M. Michajłow, A. Pręgowska, *An investigation of the dynamic electromechanical coupling effects in machine drive systems driven by asynchronous motors*, Mech. Syst. Signal Process., Vol.49 (2014) 118-134.
11. R. Konowrocki, T. Szolc, A. Pochanke, A. Pręgowska, *An influence of the stepping motor control and friction models on precise positioning of the complex mechanical system*, Mech. Syst. Signal Process., Vol.70-71 (2016) 397-413.
12. K.L., Shi, T.F., Chan, Y.K., Wong, L.S Ho, *Modelling and simulation of the three-phase induction motor using Simulink*, Int. J. Elect. Eng. Edu., 36 (1999)163-172
13. L. Lipiński, *Applying simulation models for operation analysis and selection of controller settings in traction drives with induction motors*, Electrical Machines - Transactions Journal, No. 1/ 94 (2012) 75-80 (in Polish).